Synthesis of polypeptides via bioinspired polymerization of in situ purified *N*-carboxyanhydrides

Ziyuan Song[a], Hailin Fu[b,c], Jiang Wang[d], Jingshu Hui[e], Tianrui Xue[e], Lazaro A. Pacheco[a], Haoyuan Yan[f], Ryan Baumgartner[e], Zhiyu Wang[a], Yingchun Xia[a], Xuefang Wang[a], Lichen Yin[g], Chongyi Chen[a], Joaquín Rodríguez-López[e], Andrew L. Ferguson[h], Yao Lin[b,c,1], and Jianjun Cheng[a,e,g,i,j,k,l,1]

[a]Department of Materials Science and Engineering, University of Illinois at Urbana–Champaign, Urbana, IL 61801; [b]Department of Chemistry, University of Connecticut, Storrs, CT 06269; [c]Polymer Program, Institute of Materials Science, University of Connecticut, Storrs, CT 06269; [d]Department of Physics, University of Illinois at Urbana–Champaign, Urbana, IL 61801; [e]Department of Chemistry, University of Illinois at Urbana–Champaign, Urbana, IL 61801; [f]Department of Biochemistry, University of Illinois at Urbana–Champaign, Urbana, IL 61801; [g]Institute of Functional Nano & Soft Materials, Jiangsu Key Laboratory for Carbon-Based Functional Materials & Devices, Collaborative Innovation Center of Suzhou Nano Science & Technology, Soochow University, 215123 Suzhou, China; [h]Institute for Molecular Engineering, University of Chicago, Chicago, IL 60637; [i]Department of Bioengineering, University of Illinois at Urbana–Champaign, Urbana, IL 61801; [j]Beckman Institute for Advanced Science and Technology, University of Illinois at Urbana–Champaign, Urbana, IL 61801; [k]Frederick Seitz Materials Research Laboratory, University of Illinois at Urbana–Champaign, Urbana, IL 61801; and [l]Carl R. Woese Institute for Genomic Biology, University of Illinois at Urbana–Champaign, Urbana, IL 61801

Edited by Kristi S. Anseth, University of Colorado Boulder, Boulder, CO, and approved April 19, 2019 (received for review January 25, 2019)

Ribozymes synthesize proteins in a highly regulated local environment to minimize side reactions caused by various competing species. In contrast, it is challenging to prepare synthetic polypeptides from the polymerization of *N*-carboxyanhydrides (NCAs) in the presence of water and impurities, which induce monomer degradations and chain terminations, respectively. Inspired by natural protein synthesis, we herein report the preparation of well-defined polypeptides in the presence of competing species, by using a water/dichloromethane biphasic system with macroinitiators anchored at the interface. The impurities are extracted into the aqueous phase in situ, and the localized macroinitiators allow for NCA polymerization at a rate which outpaces water-induced side reactions. Our polymerization strategy streamlines the process from amino acids toward high molecular weight polypeptides with low dispersity by circumventing the tedious NCA purification and the demands for air-free conditions, enabling low-cost, large-scale production of polypeptides that has potential to change the paradigm of polypeptide-based biomaterials.

polypeptide | *N*-carboxyanhydride | bioinspired polymerization | segregation | in situ purification

Nature has developed incredibly efficient and remarkable machinery for the synthesis of biomacromolecules, which proceeds in a complex, all-inclusive cellular environment (1). In contrast, it has been long envisioned in synthetic polymer chemistry that controlled polymerization has to be carried out from pure chemical building blocks under conditions excluding competing components (2). For instance, controlled radical polymerization is carried out in the absence of oxygen and other radical-active species to minimize undesirable chain terminations and chain transfers (3). For a similar reason, living ionic polymerization is conducted in an environment free of water and ionic impurities (4).

Proteins are synthesized through ribozyme-catalyzed linkage of amino acids under mild physiological conditions containing water, salts, and numerous other molecules (5, 6). However, the preparation of polypeptides, which are regarded as the synthetic mimics of proteins (7–15), requires prepurification of *N*-carboxyanhydride (NCA) monomers and stringent water-free polymerization conditions (16). Until now, it has remained challenging to achieve efficient and controlled polymerization of NCAs in the presence of competing species, which induce unwanted side reactions that lead to ill-defined polypeptides (17–20).

During the translation process, the ribozyme utilizes both segregation and fast reaction strategies to ensure efficient peptide bond formation and minimize the impact of competing species, which gives insights into the preparation of synthetic polypeptides. Specifically, ribosomal RNA (rRNA) provides an isolated site, peptidyl transferase center (PTC), to accommodate aminoacyl transfer RNA (tRNA) and peptidyl tRNA for the amidation reaction. The PTC not only excludes bulk water and other molecules from the reaction site (i.e., segregation) (21) but also binds and organizes the substrates for rate acceleration (22). As a result, the amino group of aminoacyl tRNA stays in its uncharged, more nucleophilic form (NH_2 instead of NH_3^+ in bulk water) (23). The peptide bond formation in ribosomes is 10^5 to 10^7 times faster than noncatalyzed amidation (22, 24), which outpaces other side reactions such as undesirable hydrolysis and allows the synthesis of high molecular weight (MW) proteins.

Inspired by the natural protein synthesis, we herein report the preparation of well-defined synthetic polypeptides from a mixture of monomers, initiators, and solvents, as well as competing species that would normally induce unwanted side reactions. We designed a water/dichloromethane (DCM) biphasic system containing interfacially anchored macroinitiators that resembles the function of rRNA, which can rapidly polymerize NCAs due to the supramolecular assembly of macroinitiators at the interface. The polymerization rate is enhanced 100-fold compared with uncatalyzed polymerization in DCM, resulting in negligible

Significance

Biomacromolecules are synthesized in cells with high precision, although the cellular environment contains numerous molecules and species other than the building blocks. In contrast, even the state-of-the-art chemical synthesis of macromolecules is exclusively carried out under a specific condition containing only clean, essential starting materials to minimize side reactions. Inspired by ribozyme-catalyzed protein synthesis, we report here controlled polypeptide synthesis by nonpurified *N*-carboxyanhydride monomers in an oil/water biphasic system that mediates impurity segregation and enables very fast polymerization that outpaces competing side reactions.

Author contributions: Z.S. and J.C. designed research; Z.S., H.F., J.W., J.H., T.X., L.A.P., H.Y., R.B., Z.W., Y.X., X.W., L.Y., C.C., J.R.-L., A.L.F., Y.L., and J.C. performed research; Z.S., H.F., Y.L., and J.C. analyzed data; and Z.S., H.F., J.W., J.H., A.L.F., Y.L., and J.C. wrote the paper.

The authors declare no conflict of interest.

This article is a PNAS Direct Submission.

[1]To whom correspondence may be addressed. Email: yao.lin@uconn.edu or jianjunc@illinois.edu.

This article contains supporting information online at www.pnas.org/lookup/suppl/doi:10.1073/pnas.1901442116/-/DCSupplemental.

Published online May 14, 2019.

water-induced monomer degradations. In addition, impurities generated during monomer synthesis, which terminate the propagating chains in conventional polypeptide synthesis, exhibited minimal inhibitory effect, due to the segregation effect. We believe this strategy not only paves the way for biomimetic synthesis of polymers but also boosts the studies and applications of polypeptide materials in various fields.

Results and Discussion

While the ester groups in tRNAs are susceptible to hydrolysis in cellular environment, ribozymes catalyze a fast amidation reaction that ensures minimal side reactions. In contrast to this process, conventional NCA polymerizations carried out in dimethylformamide or tetrahydrofuran (THF) have a comparable or even slower rate than water-induced NCA hydrolysis and polymerization (19) (*SI Appendix*, Fig. S1). Water is rigorously removed from conventional NCA polymerization medium, which would otherwise lead to low yields and ill-defined polypeptides. To get controlled NCA polymerization in the presence of water, it is essential to polymerize NCAs at a much faster rate. We recently discovered that NCA polymerization can proceed at a greatly accelerated rate by local enrichment of initiators in DCM (25). An array of polypeptide initiators adopting α-helical conformations along a linear polynorbornene backbone polymerizes NCAs at a rate 3 to 4 orders of magnitude higher than a single-chain analog, mainly due to the cooperative interactions of macrodipoles between the neighboring α-helices. Considering the immiscibility of water and DCM, we designed interfacially anchored, closely packed α-helical initiators to catalyze NCA polymerization in a water/DCM biphasic system.

To test our hypothesis that interfacially assembled helices can accelerate the NCA polymerization, we prepared methoxy poly(ethylene glycol)-*block*-poly(γ-benzyl-L-glutamate) amine (PEG–PBLG; PEG = 5 kDa, PBLG = 9.8 kDa), an amphiphilic diblock copolymer bearing an amino terminus, as the macroinitiator for NCA polymerization in the presence of water (Fig. 1*A* and *SI Appendix*, Fig. S2). Given their strong tendency to localize at the water/DCM interface, the PEG segments function as the designated interfacial anchors (26), while the hydrophobic PBLG segments fold to α-helical arrays protruding into DCM phase as the macroinitiators (Fig. 1*B*). We first prepared the water-in-oil (w/o) emulsion containing PEG–PBLG by sonicating a DCM solution of PEG–PBLG and an aqueous buffer (pH = 7.0) at a water:DCM ratio of 1:50 (wt/wt). The resulting emulsion was stable for at least 4 h with no phase separation observed (*SI Appendix*, Fig. S3), suggesting the interfacial activity of macroinitiators. The emulsion was then mixed with an equal volume of a DCM solution of purified γ-benzyl-L-glutamate NCA (BLG NCA) to start the polymerization ($[M]_0$ = 50 mM, $[I]_0$ = 0.5 mM). The polymerization proceeded rapidly and completed within 20 min, with >99% of monomer conversion (Fig. 1*E* and *SI Appendix*, Fig. S4). Gel permeation chromatography (GPC) analysis of the PEG–PBLG-initiated polymers revealed a narrow, monomodal peak with an obtained MW M_n = 37.0 kDa (Fig. 1*F*), agreeing well with the designed MW (36.8 kDa). The dispersity ($Đ = M_w/M_n$) of the resulting polypeptides was very low (~1.05), indicating excellent control throughout the polymerization process. In comparison, monomer consumption was much slower in the absence of macroinitiators under identical conditions (*SI Appendix*, Fig. S5), validating our rate enhancement design to outpace water-induced side reactions.

The importance of each block in PEG–PBLG was revealed by running control polymerizations under similar conditions, with amine-terminated PEG and PBLG as the macroinitiators. Polymerization initiated by interfacially anchored PEG showed a medium polymerization rate, reaching 95% conversion after 1 h (Fig. 1 *C* and *E*). An obviously slow, first nucleation stage within the first 10 min was observed, corresponding to the growth of random-coiled polypeptides (25). To achieve rapid polymerization kinetics, a preexisting α-helical PBLG block on macroinitiators is critical to skip the nucleation stage. Moreover, much broader dispersity and multimodal GPC curves were observed for PEG-initiated polymerization (M_n = 88.8 kDa, $Đ$ = 1.42; Fig. 1*F*), suggesting the critical role of PBLG blocks in controlling the polymerization process. On the other hand, PBLG macroinitiators would stay in the DCM phase rather than at the interface, due to the absence of PEG anchoring segments (Fig. 1*D*), which leads to slower polymerization because of increased distances between initiators. The polymerization initiated by PBLG proceeded at a much reduced rate, with ~75% monomer conversion after 2 h (Fig. 1*E*). As a result, some monomers were consumed by competitive water-induced side reactions, resulting in multimodal GPC distributions (M_n = 26.8 kDa, $Đ$ = 1.20; Fig. 1*F*).

The different interfacial anchorings of the three macroinitiators were compared by using molecular dynamics simulation. The potential of mean force (PMF) profile was computed

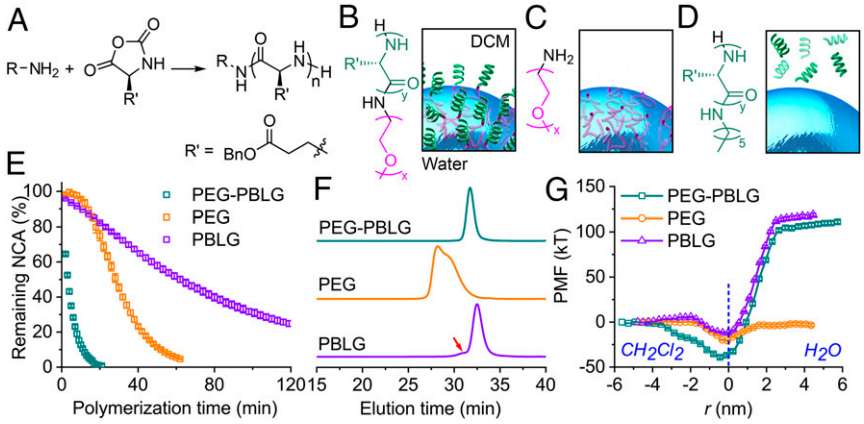

Fig. 1. Accelerated polymerization rate with localized initiators. (*A*) Scheme illustrating the polymerization of BLG NCA using three macroinitiators. (*B–D*) Chemical structure and proposed interfacial anchoring behavior of (*B*) PEG–PBLG, (*C*) PEG, and (*D*) PBLG. (*E*) Conversion of purified BLG NCA in a w/o emulsion in the presence of three macroinitiators. Polymerization condition: $[M]_0$ = 50 mM, $[I]_0$ = 0.5 mM, water:DCM = 1:100 (wt/wt). Results represent means ± SD of three replicates. (*F*) Normalized GPC-light scattering traces of resulting polymers from the polymerization initiated by three macroinitiators. Red arrow indicates the shoulder peak from PBLG-initiated polymerization. (*G*) PMF profiles of PEG–PBLG, PEG, and PBLG in a DCM/water biphasic system computed using molecular dynamics simulation. Error bars correspond to estimated SD using the bootstrap method.

using umbrella sampling for the translocation of PEG–PBLG, PEG, and PBLG from the DCM phase across the interface into the water phase (27). Mapping the relative thermodynamic favorability to exist at each location along this pathway, the deep free energy well for PEG–PBLG at the water/DCM interface reveals a thermodynamic preference to adsorb to the interface and large free energy costs associated with moving PEG–PBLG into either DCM (+35 kT) or water (+140 kT) (Fig. 1*G*). From the PMF results, the probability of staying at the interface is 100%, 94%, and 9.6% for PEG–PBLG, PEG, and PBLG, respectively (*SI Appendix*, Fig. S6), suggesting the importance of using PEG to anchor the macroinitiators at the interface. The critical role of PEG segments in stabilizing interfacial adsorption is clearly illustrated in a simulation in which a PEG–PBLG molecule in DCM is rapidly dragged toward the water/DCM interface (*SI Appendix*, Fig. S6 and Movie S1), corresponding to the most stable location of the molecule at the deep minimum of the PMF (Fig. 1*G*).

Another common side reaction encountered during NCA polymerization is the chain termination. During phosgenation of amino acids, impurities such as hydrogen chloride (HCl) and acyl chloride are generated (28–30). These acidic or electrophilic impurities, when present in even trace amounts, can protonate or react with the nucleophilic amino chain propagating species, resulting in low yields and a poorly controlled polymerization (18–20). Tedious NCA purifications by repetitive recrystallization (29) or flash column chromatography (31) under anhydrous conditions are thus inevitable. As a comparison, the segregation effect created by ribozymes ensures the nucleophile on amino-acyl tRNA remains in its deprotonated form, which facilitates the peptide bond formation. Inspired by the natural segregation strategy, we reasoned that the impurities from NCA synthesis have a strong preference to partition into aqueous phase (32), leaving only reaction-essential components (i.e., NCA monomers and amino propagating chains) in DCM phase for polymerization. Indeed, HCl shows a large partition coefficient in water/DCM ($P = 79 \pm 10$, *SI Appendix*, Fig. S7). While several synthetic polymerization systems have adopted the segregation strategy to synthesize high MW polymers with low dispersity (33, 34), it is rare to use segregation for in situ purification of starting materials.

We prepared nonpurified NCAs by skipping the moisture-free setups and tedious purification procedures (see *Materials and Methods* for more details). Due to the circumvention of purification steps, nonpurified BLG NCAs were obtained with higher isolation yield (>95%, compared with 60 to 80% after purification) in much shorter time (~5 h, while NCA purification takes days to complete). Chlorine analysis confirmed the existence of trace amount of impurities (see *SI Appendix* for more details). The impurities in nonpurified BLG NCAs significantly inhibit the polymerization with a conventional polypeptide synthesis method. When nonpurified BLG NCAs were mixed with initiators in DCM under anhydrous conditions, less than 15% NCA conversion was observed after 12 h (*SI Appendix*, Fig. S8).

To check the ability of our DCM/water biphasic system to remove NCA impurities in situ, the obtained nonpurified BLG NCAs were first treated with aqueous buffer (pH = 7.0) to promote the segregation process. A w/o emulsion containing interfacially anchored PEG–PBLG macroinitiators was then added into the biphasic mixture to start the polymerization (Fig. 2*A*; see *Materials and Methods* and Movie S2 for detailed procedures). Over 99% of nonpurified BLG NCAs was consumed within 20 min (Fig. 2*B*), indicating the critical role segregation plays in extracting the impurities. Polypeptides with high MW and low dispersity ($M_n = 37.4$ kDa, $Đ = 1.06$) were obtained from nonpurified NCAs, demonstrating the remarkable impurity tolerance of our polymerization system. NMR and Fourier transform infrared characterization revealed spectra of resulting polymers comparable to those prepared from purified NCAs under anhydrous conditions (*SI Appendix*, Fig. S9), suggesting their similar molecular structures and secondary structures. This bioinspired polymerization strategy, namely SIMPLE (Segregation-Induced Monomer-Purification and initiator-Localization promoted rate-Enhancement), avoids the stringent moisture-free setups and tedious monomer purification steps in conventional polypeptide synthesis, therefore allowing the preparation of polypeptides in a much faster and simpler manner. Well-defined polypeptides can be synthesized in gram scale within 30 min with 89% isolation yield (*SI Appendix*, Fig. S10). Conversely, conventional solution polymerization of nonpurified BLG NCA was carried out under anhydrous conditions with PEG–PBLG as macroinitiators. As expected, slow consumption of NCA was observed (<15% after 12 h) with no

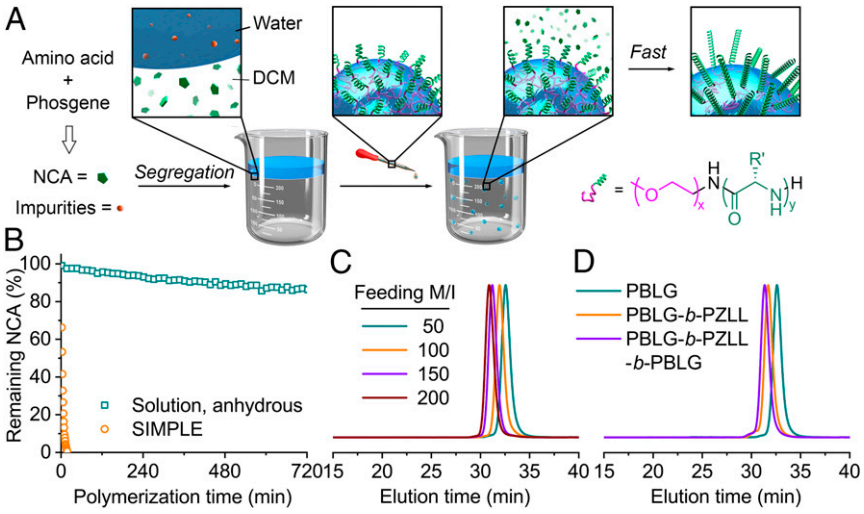

Fig. 2. SIMPLE polymerization of nonpurified NCAs. (*A*) Schematic representation showing the experimental procedures of SIMPLE polymerization of nonpurified NCAs in a water/DCM biphasic system. (*B*) Conversion of nonpurified BLG NCA initiated by PEG–PBLG in a DCM solution under anhydrous conditions and a water/DCM biphasic system (SIMPLE). Polymerization condition: $[M]_0 = 50$ mM, $[I]_0 = 0.5$ mM, water:DCM = 1:10 (wt/wt), pH = 7.0. (*C*) Normalized GPC-light scattering (LS) traces of resulting polymers from SIMPLE polymerization of nonpurified BLG NCAs at various feeding $[M]_0/[I]_0$ ratios. (*D*) Normalized GPC-LS traces of resulting block copolymers from SIMPLE polymerization through sequential addition of nonpurified monomers.

formation of high MW polypeptides (Fig. 2*B*), presumably resulting from the inhibitory effects of impurities on NCA polymerization. By varying the feeding $[M]_0/[I]_0$ ratio, we were able to control the MWs of the resulting polypeptides from nonpurified BLG NCAs (Fig. 2*C* and Table 1). In addition to PBLG, high MW poly(ε-carboxybenzyl-$_L$-lysine) and poly(γ-ethyl-$_L$-glutamate) were prepared from corresponding nonpurified NCAs with the SIMPLE method (Table 1 and *SI Appendix*, Fig. S11). Moreover, block copolymers were successfully obtained through sequential addition of nonpurified NCA monomers, confirming the livingness of the SIMPLE polymerization process (Fig. 2*D*, Table 1, and *SI Appendix*, Fig. S11).

Our previous study shows the presence of helical macrodipoles in proximity to growing chains drastically accelerates the polymerization of NCAs (25), which can be described by a two-stage, cooperative polymerization model (35–37). The self-assembly of PEG–PBLG macroinitiators at the water/DCM interface induces a similar cooperative polymerization process. To obtain more insights into the SIMPLE polymerization process, we extend the model to rationalize the experimental kinetics and the molecular distributions of the resulting polymers, by considering the multiple, competing pathways occurring at the water/DCM interface as well as in the DCM phase. For the reactions initiated by amine-capped PEG (Fig. 3*A*), most PEG chains accumulate at the water/DCM interface as suggested by the molecular simulation (Fig. 1*G*). Polymerization of NCAs starts from these anchored macroinitiators with a modest rate constant k_1 in the early stage. We note here that the initiation step may have a slightly faster rate constant (k_i) than k_1, but can be regarded as essentially of the same order. Once a critical length is reached (nucleus size $s \approx 10$, based on our previous study), however, the growing polypeptide chains fold into stable α-helices possessing strong macrodipoles. The chain propagation then proceeds with a larger rate constant k_2, facilitated by the cooperative effect of the α-helical macrodipoles assembled at the interface (25). For the polymerization initiated from PEG–PBLG (denoted as PEG-M_l* in Fig. 3*B*), the chain propagation proceeds directly into the second stage with the rate constant k_2, as augmented by the preexisting helix (with a degree of polymerization of l larger than 10) in the macroinitiator. One assumption in the model is that the polymers initiated from PEG-based initiators stay at the interface, which is justified by the deep free energy well for PEG and PEG–PBLG at the water/DCM interface (Fig. 1*G*). On the other hand, the central off-pathway reaction to be considered is the water-induced polymerization of NCAs from the w/o interface (Fig. 3*C*). The water-initiated polymerization at the interface is described analogously as PEG initiator, with the identical rate constants k_1 and k_2 in two successive growth stages, and only differs in the initiation rate constant k'_i (Fig. 3*C*). However, since the confinement of PBLG at the water/DCM interface is relatively weak (*SI Appendix*, Fig. S6), the water-initiated chains tend to diffuse back into DCM, where the chain propagation then proceeds at a rate constant (k'_2) similar to that in DCM phase, due to lack of strong cooperative effects in the molecularly dispersed state. By considering all these desired and undesired pathways, it is straightforward to write the kinetic equations corresponding to the schemes (see *SI Appendix* for more details), and find numerical solutions to them.

The multipathway model was applied to the data generated from different macroinitiators (PEG and PEG–PBLG) and the control experiment (water) (Fig. 1*E* and *SI Appendix*, Fig. S5). The optimized fits shown in Fig. 3*D*, all based on an identical set of rate constants, demonstrate an excellent agreement between the model prediction and the experimental results. Comparing k_2 and k'_2 reveals that the rate constant increases about 100-fold in magnitude from 0.075 $M^{-1}{\cdot}s^{-1}$ in DCM phase to 7.6 $M^{-1}{\cdot}s^{-1}$ at the water/DCM interface. Apparently, a strong cooperative behavior is induced at the interface where the helical macrodipoles are in close proximity. Based on the obtained kinetic parameters, the MW distributions of the polymers were predicted for different macroinitiators (Fig. 3*E*), which trend well with values obtained from GPC characterization (Fig. 1*F* and *SI Appendix*, Fig. S5). In addition, our analysis suggests that 10% of NCA monomers were consumed by water-initiated chains when PEG was used as the macroinitiator, and the percentage drastically diminished to less than 0.1% with PEG–PBLG (Fig. 3*F*). Therefore, the chain growth from PEG or PEG–PBLG at the interface can easily outpace undesirable water-induced reactions. Particularly, the use of PEG–PBLG with preexisting helices allows for the propagation kinetics to directly enter the accelerated stage, resulting in the polymers with an extremely narrow dispersity. The model was also applied to analyze SIMPLE polymerization of nonpurified NCAs initiated by PEG–PBLG (*SI Appendix*, Fig. S12), where water-initiated side reactions still only account for <1% of monomer consumption.

The interfacial anchoring of macroinitiators is not the only way to achieve fast kinetics for SIMPLE polymerization. An enhanced polymerization rate was also reported in solution phase when initiators are properly designed (25, 38). When the DCM solution of polynorbornene-derived, brush-like initiators (PNB) (25) was added into a DCM/water biphasic system containing nonpurified BLG NCAs (Fig. 4*A* and *SI Appendix*, Fig. S13), >99% NCA conversion was observed within 25 min that outpaced water-induced side reactions (Fig. 4*B*). After backbone cleavage, homopolypeptides with tunable MWs and low $Đ$ (<1.15) were obtained (Fig. 4*C*). The higher MWs than expected values are attributed to the two-stage kinetics, which inevitably generate low MW oligomers (37). In addition, polypeptides with tunable MWs were also obtained with Tris(2-aminoethyl)amine as the initiator, which exhibited fast polymerization kinetics due to the activation of NCA monomers (*SI Appendix*, Fig. S14) (38). To validate that the rapid polymerization kinetics is critical to minimize water-induced side reactions, control polymerizations were carried out in the presence of 1-pyrenemethyl amine without a rate acceleration mechanism. GPC analysis revealed that almost all high MW polypeptides were initiated by water, while pyrene signal was only observed in some oligomeric species (*SI Appendix*, Fig. S14).

Inspired by the natural protein synthesis, we developed here SIMPLE, a rare example of controlled polymerization in an open system capable of in situ monomer purification. This polymerization approach allows the synthesis of well-defined polypeptides that completely eliminates NCA purification steps and the need for moisture-free setups, some of the outstanding challenges for

Table 1. Polymerization results of nonpurified NCA monomers by SIMPLE

Monomer	$[M]_0/[I]_0$	t/min[†]	M_n(M_n*)/kDa[‡]	$Đ$
BLG	50	12	24.4(25.8)	1.06
	100	16	37.4(36.8)	1.06
	150	18	48.0(47.8)	1.05
	200	19	55.5(58.7)	1.05
ZLL	100	13	44.3(41.1)	1.07
ELG	100	30	29.9(30.6)	1.06
BLG/ZLL/BLG[§]	50	7	23.7(25.8)	1.06
	50	6	34.8(36.8)	1.09
	50	16	42.8(45.7)	1.09

All polymerizations were conducted in a water/DCM biphasic system in the presence of PEG–PBLG macroinitiators. $[I]_0$ = 0.5 mM except for the last three entries. ELG, γ-ethyl-$_L$-glutamate; ZLL, ε-carboxybenzyl-$_L$-lysine.
[†]Polymerization time reaching 98% monomer conversion.
[‡]Obtained MW (designed MW*).
[§]Synthesis of block copolymer through sequential monomer addition. $[I]_0$ = 1.0, 0.5, and 0.25 mM for the first, second, and third block, respectively.

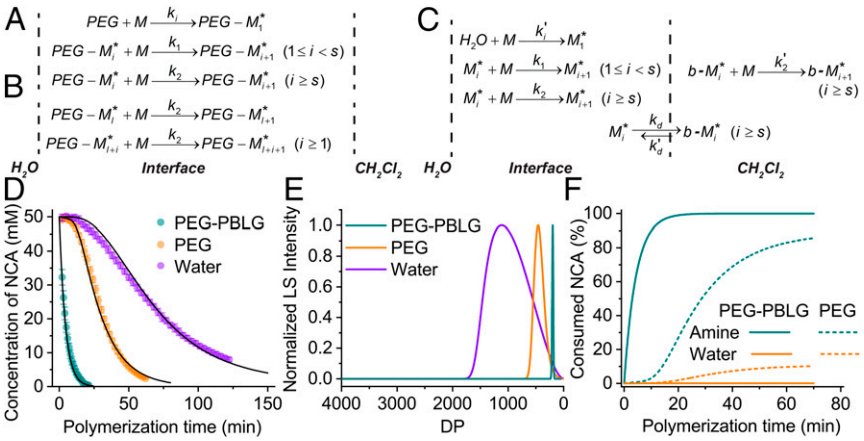

Fig. 3. Kinetic modeling of SIMPLE polymerization. (*A*–*C*) Schematic representation of two-stage kinetic model for NCA polymerization in a w/o emulsion, including (*A*) PEG-initiated polymerization, (*B*) PEG–PBLG-initiated polymerization, and (*C*) water-induced polymerization. An active polymer with DP = *i* is denoted as M_i*; *b*-M_i* represents the active polymer in the bulk DCM phase. (*D*) Kinetic data from various initiators (colored circles) were fit with the cooperative kinetic model (black lines). Rate constants were determined as follows: $k_i = k_1 = 0.24\ M^{-1}{\cdot}s^{-1}$, $k_2 = 7.6\ M^{-1}{\cdot}s^{-1}$, $k'_i[H_2O] = 4.5 \times 10^{-7}\ s^{-1}$, $k_d = 1.3 \times 10^{-4}\ s^{-1}$, and $k'_2 = 0.075\ M^{-1}{\cdot}s^{-1}$. For simplicity, we assume the initiation rate constant equals the propagation rate constant in the coiled state ($k_i = k_1$), as they have similar propagating structures. In addition, we assume water-initiated PBLG with a DP > *s* has an irreversible diffusion from the interface to oil phase ($k'_d = 0$). (*E*) Simulated GPC-light scattering traces from various initiators predicted by the kinetic model. (*F*) Prediction of water competition in PEG–PBLG- and PEG-initiated polymerization in a w/o emulsion.

the synthesis of polypeptides via NCAs. The preparation of polypeptide materials has been substantially simplified, which makes it possible to prepare polypeptides from hard-to-purify NCAs and opens the door for easy synthesis of polypeptides.

Materials and Methods

Detailed experimental procedures and characterization of compounds can be found in *SI Appendix*.

Synthesis of Purified and Nonpurified NCAs. Anhydrous solvents were used for the synthesis and purification of purified NCAs; regular solvents (stored over anhydrous Na_2SO_4) were used for the synthesis of nonpurified NCAs. Take BLG NCA as an example: BLG (2.0 g, 8.4 mmol) was added into a flame-dried 250-mL Schlenk flask charged with a stir bar, and the amino acid was dried under vacuum for 2 h. Anhydrous THF (30 mL) was then added into the flask, and the flask was cooled down to 0 °C with an ice bath. Toluene solution of phosgene (15 wt%, 7.2 mL, 10.1 mmol of phosgene, 1.2 equiv.) was added, and the mixture was stirred at 50 °C for 2 h. After the solution was cooled down to room temperature, THF and residual phosgene was removed under vacuum. (Note that phosgene is extremely toxic and should be handled with care. The residues in the cold trap need to be neutralized with saturated aqueous solution of $NaHCO_3$.) The crude product was recrystallized three times at room temperature from anhydrous THF/hexane (1:4, vol/vol). The product BLG NCA was obtained as white needle-like crystals after drying under vacuum, and stored in a glove box at −30 °C. Isolated yield was 72 to 78%. Nonpurified BLG NCA was prepared in a similar way to purified BLG NCA, but without the steps of vacuum drying of amino acids and recrystallization. The amount of phosgene used was 1.3 equiv. compared with BLG. After the removal of solvent THF and residual phosgene, the solid residues were dissolved in DCM, transferred into a 20-mL vial, and dried. Isolated yield was 96 to 98%.

SIMPLE Polymerization. SIMPLE polymerization was conducted in a flat-bottom 7- or 20-mL glass vial (milligram scale synthesis) or a round-bottom 50-mL flask (gram scale synthesis). Typically, a w/o emulsion containing PEG–PBLG macroinitiators (1 mM) was prepared by emulsifying a mixture of a regular DCM solution of PEG–PBLG macroinitiators and an aqueous buffer (pH = 7.0, 2 wt%). To promote segregation-induced in situ purification, nonpurified NCAs were dissolved in regular DCM (0.1 M), mixed with aqueous buffer (pH = 7.0, 18 wt%), and vortexed for 10 s. The w/o emulsion containing PEG–PBLG was then immediately added into the mixture to start the polymerization. Final condition was $[M]_0 = 50$ mM, $[I]_0 = 0.5$ mM, water:DCM = 1:10, wt/wt.

Molecular Dynamics Simulation. All-atom molecular models of PEG–PBLG, PEG, PBLG, and DCM solvent were generated using the Automated Topology Builder server (http://atb.uq.edu.au) (39) and modeled using the Groningen Molecular Simulation (GROMOS) 54A7 force field (40). Molecular dynamics simulations were conducted using the Groningen Machine for Chemical Simulations (GROMACS) 4.6 simulation suite (41). Simulation trajectories were

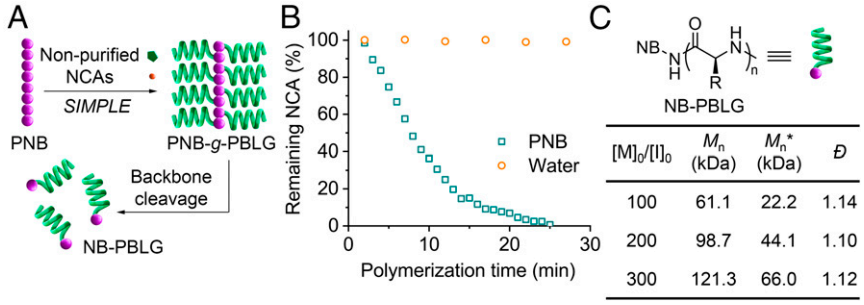

$[M]_0/[I]_0$	M_n (kDa)	M_n* (kDa)	$Đ$
100	61.1	22.2	1.14
200	98.7	44.1	1.10
300	121.3	66.0	1.12

Fig. 4. Extension of SIMPLE concept. (*A*) Scheme illustrating the synthesis of homopolypeptides from nonpurified NCAs in the presence of water, which was achieved by SIMPLE polymerization using a PNB followed by a backbone cleavage step. (*B*) Conversion of nonpurified BLG NCA initiated by PNB in a water/DCM biphasic system. $[M]_0 = 50$ mM, $[M]_0/[I]_0 = 100$, water:DCM = 1:10 (wt/wt). (*C*) GPC characterization of homopolypeptides (NB–PBLG) after backbone cleavage.

visualized using Visual Molecular Dynamics (42). Umbrella sampling simulation (27) and Weighted Histogram Analysis Method (43, 44) were conducted to calculate the PMF of molecules crossing the water/DCM interface.

Kinetic Modeling. The differential equations were solved numerically using ode15s in Matlab, with s set to be 10 and k'_2 predetermined by analyzing PBLG-initiated polymerization of BLG NCA in DCM solution (*SI Appendix*, Fig. S12*A*). Rate constants k'_i, k_1, k_2, and k_d were obtained by globally fitting the kinetic profiles under different initiation mechanisms (Fig. 3*D*). Based on the obtained rate constants, the MW distributions of polypeptides under different experimental conditions were simulated by solving the set of differential equations numerically. The predicted MW distributions were converted into normalized light scattering intensity by assuming all helices as rigid rods and by applying the Guinier approximation (45).

Data Availability. The authors declare that the main data supporting the findings of this study are available within the paper and *SI Appendix*.

ACKNOWLEDGMENTS. This work was supported by National Science Foundation under Awards CHE-1709820 (to J.C.), DMR-1809497 (to Y.L.), and DMS-1841810 (to A.L.F.), and National Institutes of Health under Award 1R01CA207584. We thank L. Zhu for assistance with NMR studies; E. S. Garcia-Ramirez and S. C. Zimmerman for access to GPC analysis; and R. Wang and K. Cai for helpful discussions.

1. Nelson DL, Lehninger AL, Cox MM (2008) *Lehninger Principles of Biochemistry* (W. H. Freeman, New York).
2. Szwarc M (1956) 'Living' polymers. *Nature* 178:1168–1169.
3. Matyjaszewski K, Davis TP (2003) *Handbook of Radical Polymerization* (John Wiley, Hoboken, NJ).
4. Szwarc M, van Beylen M (1993) *Ionic Polymerization and Living Polymers* (Springer, Dordrecht, The Netherlands).
5. Schmeing TM, Ramakrishnan V (2009) What recent ribosome structures have revealed about the mechanism of translation. *Nature* 461:1234–1242.
6. Rodnina MV (2011) Mechanisms of decoding and peptide bond formation. *Ribosomes: Structure, Function, and Dynamics*, eds Rodnina MV, Wintermeyer W, Green R (Springer, Vienna), pp 199–212.
7. Krejchi MT, et al. (1994) Chemical sequence control of beta-sheet assembly in macromolecular crystals of periodic polypeptides. *Science* 265:1427–1432.
8. Kukula H, Schlaad H, Antonietti M, Förster S (2002) The formation of polymer vesicles or "peptosomes" by polybutadiene-*block*-poly($_L$-glutamate)s in dilute aqueous solution. *J Am Chem Soc* 124:1658–1663.
9. Bellomo EG, Wyrsta MD, Pakstis L, Pochan DJ, Deming TJ (2004) Stimuli-responsive polypeptide vesicles by conformation-specific assembly. *Nat Mater* 3:244–248.
10. Rodríguez-Hernández J, Lecommandoux S (2005) Reversible inside-out micellization of pH-responsive and water-soluble vesicles based on polypeptide diblock copolymers. *J Am Chem Soc* 127:2026–2027.
11. Deming TJ (1997) Facile synthesis of block copolypeptides of defined architecture. *Nature* 390:386–389.
12. Petka WA, Harden JL, McGrath KP, Wirtz D, Tirrell DA (1998) Reversible hydrogels from self-assembling artificial proteins. *Science* 281:389–392.
13. Nowak AP, et al. (2002) Rapidly recovering hydrogel scaffolds from self-assembling diblock copolypeptide amphiphiles. *Nature* 417:424–428.
14. Gabrielson NP, et al. (2012) Reactive and bioactive cationic α-helical polypeptide template for nonviral gene delivery. *Angew Chem Int Ed Engl* 51:1143–1147.
15. Lam SJ, et al. (2016) Combating multidrug-resistant Gram-negative bacteria with structurally nanoengineered antimicrobial peptide polymers. *Nat Microbiol* 1:16162.
16. Katchalski E, Sela M (1958) Synthesis and chemical properties of poly-α-amino acids. *Advances in Protein Chemistry*, eds Anfinsen CB, Anson ML, Bailey K, Edsall JT (Academic, San Diego), Vol 13, pp 243–492.
17. Bartlett PD, Jones RH (1957) A kinetic study of the Leuchs anhydrides in aqueous solution. I. *J Am Chem Soc* 79:2153–2159.
18. Aliferis T, Iatrou H, Hadjichristidis N (2004) Living polypeptides. *Biomacromolecules* 5:1653–1656.
19. Hadjichristidis N, Iatrou H, Pitsikalis M, Sakellariou G (2009) Synthesis of well-defined polypeptide-based materials via the ring-opening polymerization of α-amino acid *N*-carboxyanhydrides. *Chem Rev* 109:5528–5578.
20. Cheng J, Deming TJ (2012) Synthesis of polypeptides by ring-opening polymerization of α-amino acid N-carboxyanhydrides. *Peptide-Based Materials*, ed Deming TJ (Springer, Berlin), pp 1–26.
21. Schmeing TM, Huang KS, Kitchen DE, Strobel SA, Steitz TA (2005) Structural insights into the roles of water and the 2′ hydroxyl of the P site tRNA in the peptidyl transferase reaction. *Mol Cell* 20:437–448.
22. Sievers A, Beringer M, Rodnina MV, Wolfenden R (2004) The ribosome as an entropy trap. *Proc Natl Acad Sci USA* 101:7897–7901.
23. Kingery DA, et al. (2008) An uncharged amine in the transition state of the ribosomal peptidyl transfer reaction. *Chem Biol* 15:493–500.
24. Trobro S, Åqvist J (2005) Mechanism of peptide bond synthesis on the ribosome. *Proc Natl Acad Sci USA* 102:12395–12400.
25. Baumgartner R, Fu H, Song Z, Lin Y, Cheng J (2017) Cooperative polymerization of α-helices induced by macromolecular architecture. *Nat Chem* 9:614–622.
26. Malzert A, et al. (2003) Interfacial properties of adsorbed films made of a PEG2000 and PLA50 mixture or a copolymer at the dichloromethane-water interface. *J Colloid Interface Sci* 259:398–407.
27. Torrie GM, Valleau JP (1977) Nonphysical sampling distributions in Monte Carlo free-energy estimation: Umbrella sampling. *J Comput Phys* 23:187–199.
28. Iwakura Y, Uno K, Kang S (1965) The synthesis and reactions of 2-isocyanatoacyl chlorides. *J Org Chem* 30:1158–1161.
29. Kricheldorf HR (1987) Synthesis and characterization of NCAs. *α-Aminoacid-N-Carboxy-Anhydrides and Related Heterocycles*, ed Kricheldorf HR (Springer, Berlin), pp 3–58.
30. Dorman LC, Shiang WR, Meyers PA (1992) Purification of γ-benzyl and γ-methyl L-glutamate N-carboxyanhydrides by rephosgenation. *Synth Commun* 22:3257–3262.
31. Kramer JR, Deming TJ (2010) General method for purification of α-amino acid-*n*-carboxyanhydrides using flash chromatography. *Biomacromolecules* 11:3668–3672.
32. Poché DS, Moore MJ, Bowles JL (1999) An unconventional method for purifying the N-carboxyanhydride derivatives of γ-alkyl-L-glutamates. *Synth Commun* 29:843–854.
33. McHale R, Patterson JP, Zetterlund PB, O'Reilly RK (2012) Biomimetic radical polymerization via cooperative assembly of segregating templates. *Nat Chem* 4:491–497.
34. Engelis NG, et al. (2017) Sequence-controlled methacrylic multiblock copolymers via sulfur-free RAFT emulsion polymerization. *Nat Chem* 9:171–178.
35. Oosawa F, Asakura S (1975) *Thermodynamics of the Polymerization of Protein* (Academic, San Diego).
36. Zhao D, Moore JS (2003) Nucleation-elongation: A mechanism for cooperative supramolecular polymerization. *Org Biomol Chem* 1:3471–3491.
37. De Greef TFA, et al. (2009) Supramolecular polymerization. *Chem Rev* 109:5687–5754.
38. Zhao W, Gnanou Y, Hadjichristidis N (2015) From competition to cooperation: A highly efficient strategy towards well-defined (co)polypeptides. *Chem Commun (Camb)* 51:3663–3666.
39. Malde AK, et al. (2011) An automated force field topology builder (ATB) and repository: Version 1.0. *J Chem Theory Comput* 7:4026–4037.
40. Schmid N, et al. (2011) Definition and testing of the GROMOS force-field versions 54A7 and 54B7. *Eur Biophys J* 40:843–856.
41. Hess B, Kutzner C, van der Spoel D, Lindahl E (2008) GROMACS 4: Algorithms for highly efficient, load-balanced, and scalable molecular simulation. *J Chem Theory Comput* 4:435–447.
42. Humphrey W, Dalke A, Schulten K (1996) VMD: Visual molecular dynamics. *J Mol Graph* 14:33–38, 27–28.
43. Kumar S, Rosenberg JM, Bouzida D, Swendsen RH, Kollman PA (1992) THE weighted histogram analysis method for free-energy calculations on biomolecules. I. The method. *J Comput Chem* 13:1011–1021.
44. Roux B (1995) The calculation of the potential of mean force using computer simulations. *Comput Phys Commun* 91:275–282.
45. Guinier A, Fournet G (1955) *Small-Angle Scattering of X-Rays* (John Wiley, New York).